

23 Stars notes 2019/10/23 - Wed - Spectra,

23.1 Physical basis for two spectral parameters

at the atmosphere, the scale height is

$$H_P = \frac{kT}{\mu m_p g} \ll R$$

so then all atmospheric calculations can be done in a plane-parallel geometry. In that geometry the only parameters are $g = GM/R^2$ and the flux F leaving in $\text{erg/cm}^2\text{-sec.}$ and the chemical abundances. We rewrite flux as

$$T_{eff} \equiv \left(\frac{F}{\sigma_{SB}} \right)^{1/4}$$

Most of what we see in spectra is variations T_{eff} and we can measure this quite well.

At the photosphere

$$\tau = 1 = \int \kappa \rho dr = \kappa y = \kappa \frac{P}{g}$$

for an ideal gas at the photosphere

$$P = \frac{\rho k T_{eff}}{\mu m_p}$$

so the number density is

$$n_{ph} \simeq \frac{m_p g}{\sigma_{Th} k_B T_{eff}}$$

for $\kappa = \kappa_{es}$ so the number density scales with gravity, the photosphere will be denser at higher gravities. Putting numbers for the Sun

$$n_{ph} \simeq 10^{16} \text{cm}^{-3} \left(\frac{10^4}{T_{eff}} \right) \left(\frac{g}{2.7 \times 10^4 \text{cm/s}^2} \right)$$

Formation of spectral lines: "absorption" lines (deficits in flux) appear because photons at line wavelength come from shallower (cooler) depth in atmosphere. Opacity, κ , is higher for photons at line wavelength, so line photosphere ($\tau = \kappa P/g = 1$) is shallower (lower P).

23.2 Spectral Sequence for Stars

Now use the Saha equation to get some sense of the spectral types.

The sequence is O B A F G K M, hot to cool. This is an effective temperature scale. There are gradations within this O1→O10, B0→B10. increasing number is colder. Also note that in some classes not all the numbers are filled in.

Additionally, Luminosity class: V = dwarf → I = supergiants.

Sp Type	T_{eff}	M/M_{\odot} (ZAMS)
O3	52,000	120
O8	36,000	23
B0	30,000	17
B5	15,400	6
A0	9520	3
G0	6030	1.05
M0	3850	0.5

The luminosity classes are really indexed by g , but it is hard to really measure this value. Sets the photospheric density.

Two spectral types for really cold dwarf (fairly recent additions) L and T classes.

Even worse: the spectral locations are referred to as Early type (OB) and Late type (KM). This from an old idea of stellar evolution.

23.3 Ionization states and spectral appearance

Really determines what the spectrum "looks" like. Quantum has to be used to set the actual temperature scale. Most of the spectral classification comes from the presence/absence of different elemental features. (Based on first ionization potential)

Alkali metals (Li, Na, Mg, Al), ≤ 5 eV

– (H, C, N, O) $10 < E < 20$ eV

Noble (He, Ne) > 20 eV

Can get a sense by following a few ionization states. Follow ionization state for (First ionization potential) FIP: H - 13.6 eV, He - 24.6 eV, Na - 5.14 eV.

For Na, $\underline{Na^+ + e^- \leftrightarrow Na + \gamma}$ which gives Saha equation

$$\frac{n_{Na^+}n_e}{n_{Na}} = \left(\frac{2\pi m_e kT}{h^2}\right)^{3/2} \exp\left(-\frac{E_i}{kT}\right)$$

taking the ratio for different species the prefactor cancels so can compare Na to H

$$\frac{n_{Na^+}}{n_{Na}} = \exp\left(-\frac{(E_{Na} - E_H)}{kT}\right) \frac{n_{H^+}}{n_H} = 10^7 \frac{n_{H^+}}{n_H}$$

and similarly for He

$$\frac{n_{He^+}}{n_{He}} = \exp\left(-\frac{(E_{He} - E_H)}{kT}\right) \frac{n_{H^+}}{n_H} = 6 \times 10^{-10} \frac{n_{H^+}}{n_H}$$

where the numbers are for the sun at $T = 6000$ K. so the Na is ionized but the He is not.

$n_e(cm^{-3})$	$T_{1/2}(Na)$	$T_{1/2}(H)$	$T_{1/2}(He)$
10^{13}	3090	8000	14500
10^{14}	3500	9082	16500
10^{15}	4057	10500	19000
10^{16}	4810	12450	22570

23.4 Showing some spectra

Figure 8.4 and 8.5 from Carroll and Ostlie show examples of various spectral types:

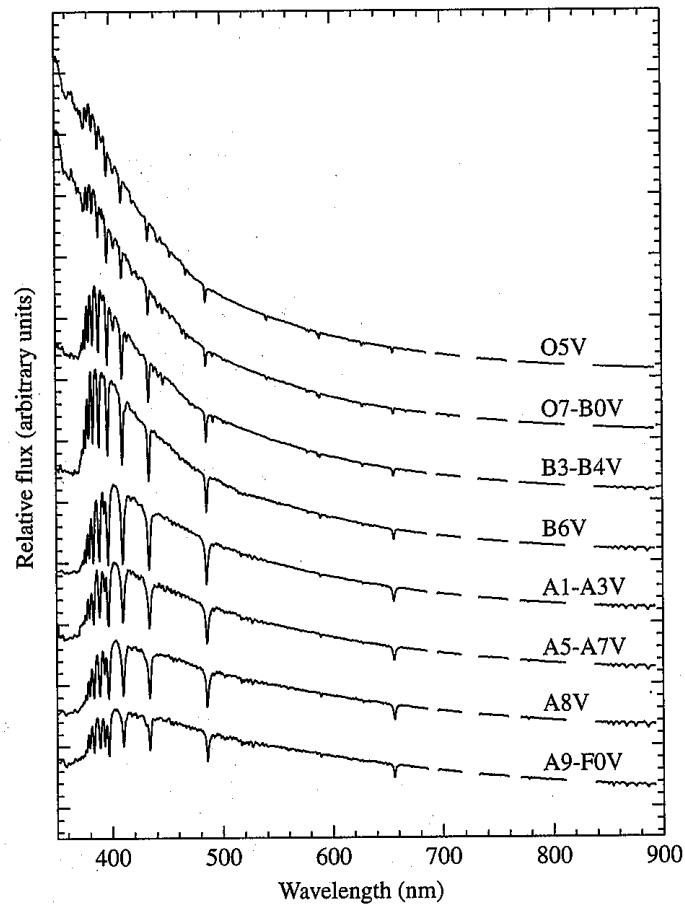


FIGURE 8.4 Digitized spectra of main sequence classes O5–F0 displayed in terms of relative flux as a function of wavelength. Modern spectra obtained by digital detectors (as opposed to photographic plates) are generally displayed graphically. (Data from Silva and Cornell, *Ap. J. Suppl.*, 81, 865, 1992.)

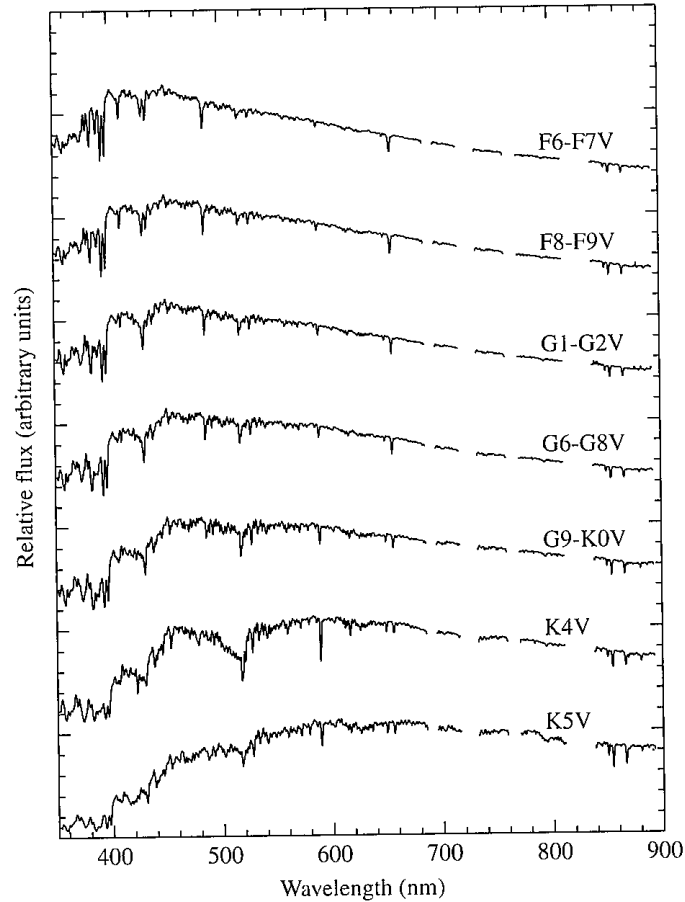


FIGURE 8.5 Digitized spectra of main sequence classes F6–K5 displayed in terms of relative flux as a function of wavelength. (Data from Silva and Cornell, *Ap. J. Suppl.*, 81, 865, 1992.)

OB Type: All H is ionized, He is either neutral or partially ionized. at late B you start to see Balmer.

A Type: H lines, ionized Mg are present.

F Type: Mostly metal lines as most H is neutral AND all in ground state.

G and K

and finally M class

spectra for L and T class:

810

KIRKPATRICK ET AL.

Vol. 519

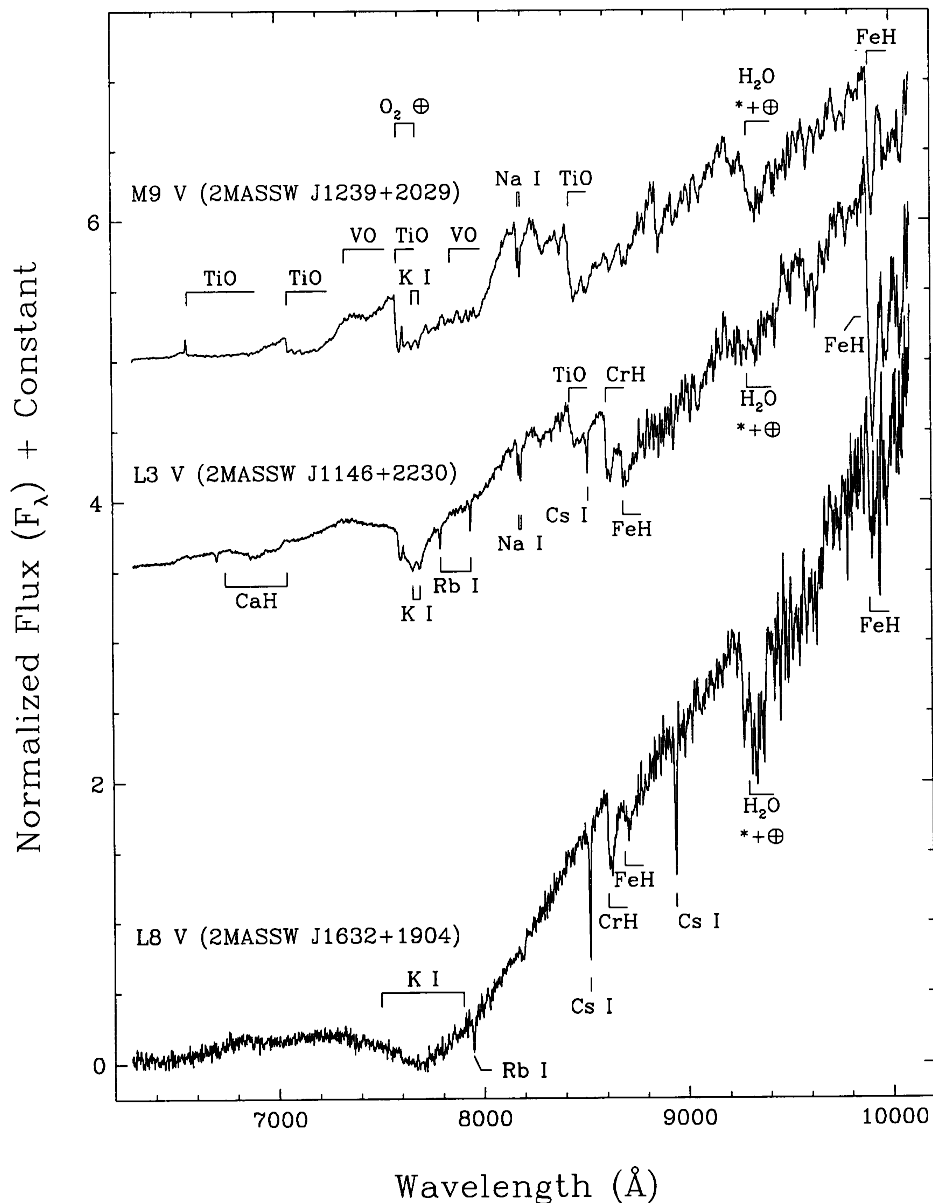


FIG. 4.—Enlarged spectra of a late-M, early- to mid-L, and late-L dwarf. Prominent features are marked. Note the absence of oxide absorption in the L dwarfs along with the dominance of alkali lines and hydride bands. Names for the 2MASS objects have been abbreviated.

dwarfs of type M7 and later, these types were refined using the VO ratio described in Kirkpatrick, Henry, & Irwin (1997b).

All dwarfs later than spectral type M9.5 are discussed in the next section, and notes on individual M9.5+ dwarfs can be found in Appendix A. Notes on other interesting objects can be found in Appendix B.

4. RESULTS FOR DWARFS COOLER THAN TYPE M9.5 V

Listed in Table 3 are all the dwarfs from Tables 1A and 2 that have spectral types cooler than M9.5 V. This includes

the 2MASS dwarf discovered in Prototype Camera data (Kirkpatrick et al. 1997a), Kelu-1 discovered during the course of the proper-motion survey of Ruiz, Leggett, & Allard (1997), and the three cool dwarfs discovered by the Deep Near Infrared Survey (DENIS; Delfosse et al. 1997; Tinney, Delfosse, & Forveille 1997). Also included in the table for comparison purposes are the only two companion objects currently known with spectral types cooler than M9.5 V: GD 165B and Gl 229B. In total, 26 dwarfs have been found with post-M9.5 types, and 20 of those are from 2MASS. Optical and near-infrared finder charts for the

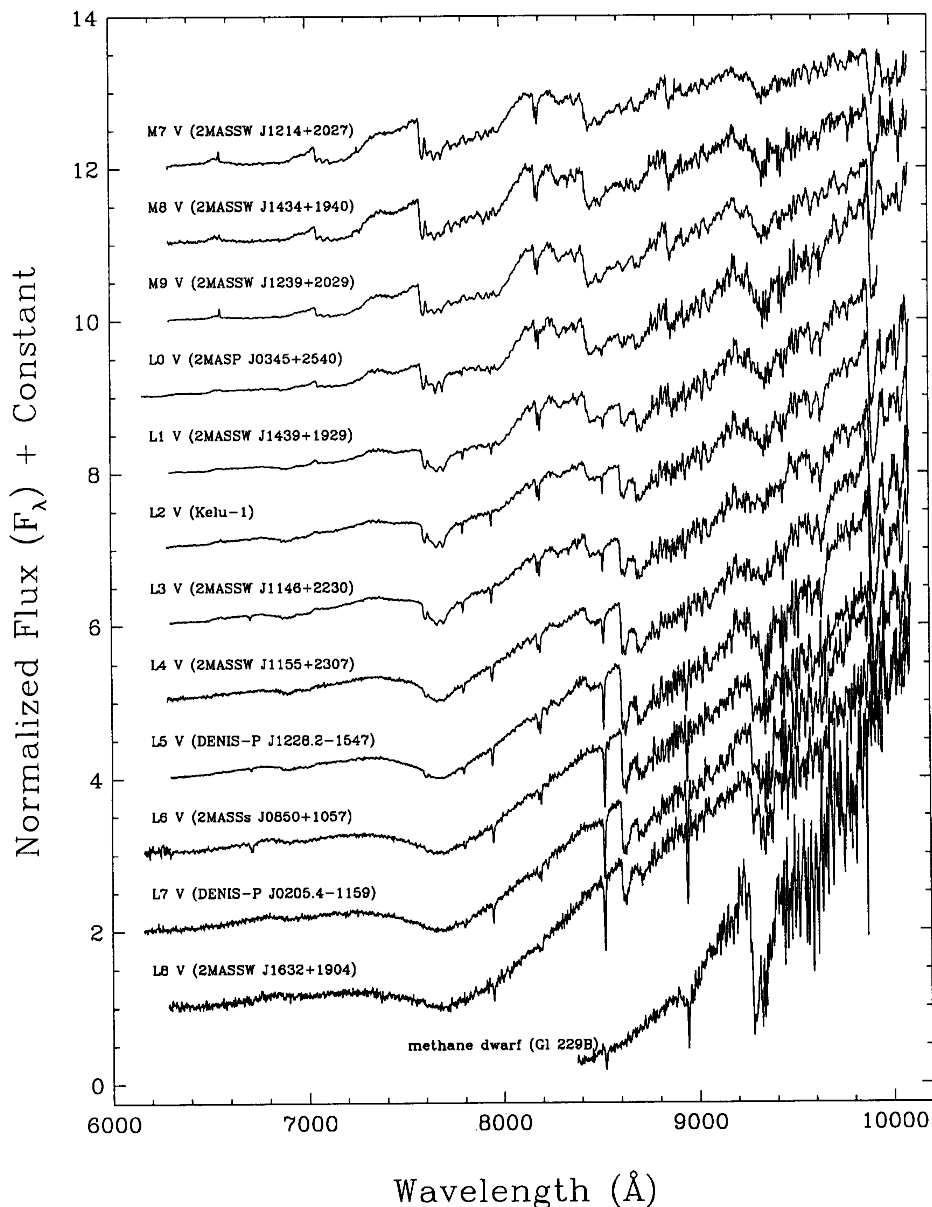


FIG. 6.—L-dwarf spectral sequence. This is a subset of the Keck LRIS data of Fig. 3, but showing only one spectrum for each subclass from L0 through L8. Also shown for comparison is the Oppenheimer et al. spectrum of GI 229B and three late-M dwarfs from Table 1A, also taken with LRIS on Keck. Again, names for the 2MASS objects have been abbreviated.

well behaved, clearly demonstrating the fact that CrH increases strength from late M through early L, reaches peak strength at L5 V, then weakens toward the latest L types.⁹ The FeH-a and FeH-b ratios show similar behavior,

⁹ As Figure 10b shows, the CrH-b ratio, which measures the CrH band at 9969 Å, is unusable as a spectral diagnostic in these data. This is because of the poor sensitivity of the CCD at this wavelength and because of the lack of a suitable continuum region.

with FeH increasing from late M through mid-L then weakening toward the latest L types.

Because the alkalis of Figure 8 and the oxides of Figure 9 show ratios for the primary standards that monotonically increase or decrease throughout the L sequence, composite alkali-oxide ratios, which serve as more sensitive discriminants, can be devised. The values for some of these ratios are shown in Figure 11, where the primary standards are again illustrated by the large dots.

definitions of spectral types L and T.

No. 2, 1999

DEFINITION OF SPECTRAL TYPE "L"

815

Kirkpatrick et al '99 ApJ 519, 802

TABLE 6
QUALITATIVE DEFINITIONS FOR L SUBCLASSES

Subclass (1)	Spectral Characteristics* (2)	Example (3)
L0	VO $\lambda\lambda$ 7400, 7900 at its strongest—7800–8000 Å portion of spectrum is flat TiO λ 8432 depth similar to both CrH λ 8611 and FeH λ 8692 TiO λ 7053 present at high signal-to-noise but weak Rb I and Cs I doublets weakly visible but strengthening	2MASS J0345432 + 254023
L1	TiO λ 8432, CrH λ 8611, FeH λ 8692 nearly equal strength; FeH deeper than CrH, CrH deeper than TiO VO $\lambda\lambda$ 7400, 7900 weakening; 7800–8000 Å portion of spectrum slightly sloped Na I doublet weakening TiO $\lambda\lambda$ 7053, 8432 weakening Rb I and Cs I doublets strengthening K I line cores broadening	2MASSW J1439284 + 192915
L2	TiO λ 8432 much weaker than CrH λ 8611 or FeH λ 8692; FeH deeper than CrH K I line cores still visible and still broadening TiO λ 8432 weaker and TiO λ 7053 vanished VO $\lambda\lambda$ 7400, 7900 weakening more: 7800–8000 portion of spectrum distinctly sloped Na I weakening; Rb I and Cs I still strengthening	Kelu-1
L3	K I still broadening with cores still weakly visible VO λ 7900 barely present as slight depression in "continuum" between 7800 and 8200 Å TiO λ 8432 still weakening Na I still weakening; Rb I and Cs I still strengthening	2MASSW J1146345 + 223053
L4	K I wings are very broad and line cores no longer visible CrH λ 8611 equal in strength to FeH λ 8692 VO λ 7900 vanished (no depression visible at all between 7800 and 8200 Å) TiO λ 8432 still weakening Na I still weakening; Rb I and Cs I still strengthening	2MASSW J1155009 + 230706
L5	CrH λ 8611 now stronger than FeH λ 8692 TiO λ 8432 very weak K I region shows broad depression Na I still weakening Rb I and Cs I still strengthening; Cs I λ 8521 less deep than CrH λ 8611	DENIS-P J1228.2 – 1547
L6	TiO λ 8432 barely perceptible K I region shows very broad depression FeH $\lambda\lambda$ 8692, 9896 and CrH λ 8611 weakening; CrH λ 8611 deeper than FeH λ 8692 Na I still weakening Rb I and Cs I still strengthening; Cs I λ 8521 now deeper than CrH λ 8611	2MASSs J0850359 + 105716
L7	TiO λ 8432 virtually gone FeH $\lambda\lambda$ 8692, 9896 and CrH λ 8611 still weakening; CrH λ 8611 still deeper than FeH λ 8692 K I region shows very broad depression Rb I and Cs I still strengthening Na I still weakening	DENIS-P J0205.4 – 1159
L8	FeH $\lambda\lambda$ 8692, 9896 very weak CrH λ 8611 still weakening though still stronger than FeH λ 8692 K I region shows very broad depression Rb I and Cs I still strengthening; Cs I λ 8521 ~2 times as deep as CrH λ 8611 Na I barely perceptible	2MASSW J1632291 + 190441

* Relative depths of bands refer to spectra with absolute flux calibrations (F_λ) similar to those in Figs. 7 and 8.

No. 2, 1999

DEFINITION OF SPECTRAL TYPE "L"

827

TABLE 11
SPECTRAL FEATURES USABLE AS L-DWARF TEMPERATURE INDICATORS

Atom or Molecule (1)	Observed Maximum (2)	Observed Disappearance (3)	Theoretical Explanation* (4)	Predicted Disappearance* (5)
TiO	~M8	~L2 ^b	Condenses into CaTiO ₃	2300–2000 K
VO	~M9	~L4	Depletes into solid VO	1700–1900 K
FeH	~L4	>L8
CrH	~L5	>L8	Converts into metallic CrH	~1400 K
Li I	~L6?	~L7?	Forms into LiCl	≤1400 K
CO	C becomes bound to CH ₄	1200–1500 K
Rb I	≥L8	...	Forms into RbCl	≤1200 K
Cs I	≥L8	...	Forms into CsCl	≤1200 K
K I	Forms into KCl	≤1200 K
Na I ^d	Forms into NaCl	~1150 K
H ₂ O	Disappears into H ₂ O condensate	~350 K

^a Taken from Burrows & Sharp 1999.
^b True for all bands except the one at 8432 Å, which doesn't disappear until about L5–6.
^c Not included in Burrows & Sharp 1999.
^d Only a higher excitation doublet, not the ground-state doublet, is included in our spectral region. See text for discussion.

23.5 Bit more on line strength

The strength of absorption features of various elements (and molecules at the low temperature end) is strongly dependent on the stellar temperature, making this a good diagnostic of the temperature. The dependence is shown in figure 8.11:

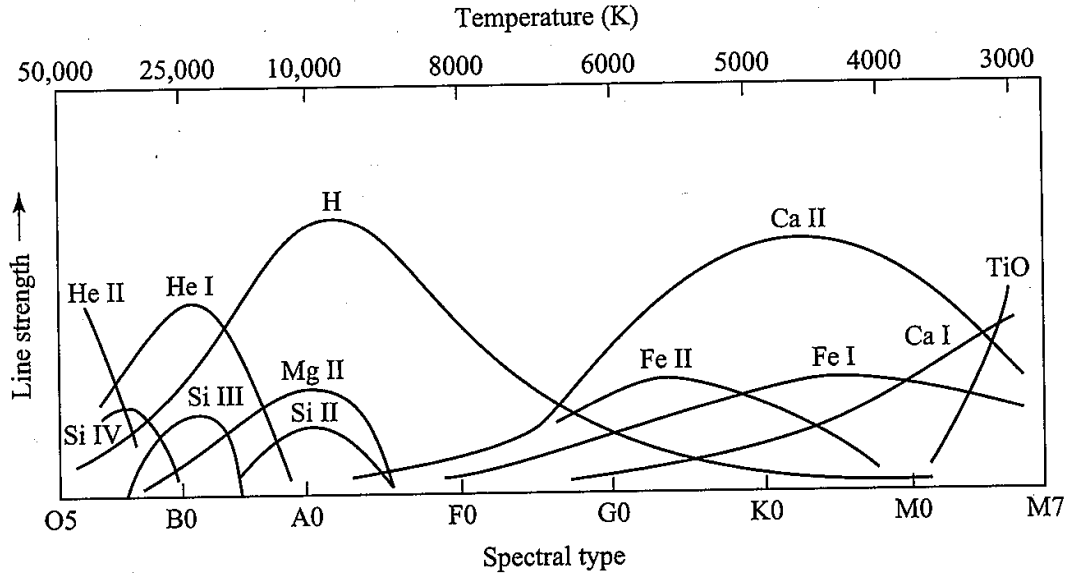


FIGURE 8.11 The dependence of spectral line strengths on temperature.

Strength of absorption features is determined by population of levels in the atoms near the photosphere. The hydrogen absorption lines in the optical are Balmer, and so based off of $n = 2$. At high temperatures, most of the H is ionized, so the lines are weak. At low temperature, most of the atoms' electrons are in $n = 1$, and so the Balmer lines are weak there as well. Their strength peaks around 8000 K, which corresponds roughly to an A star.

Surface gravity is measured by luminosity classes: V is highest gravity, I is lowest gravity = largest star.

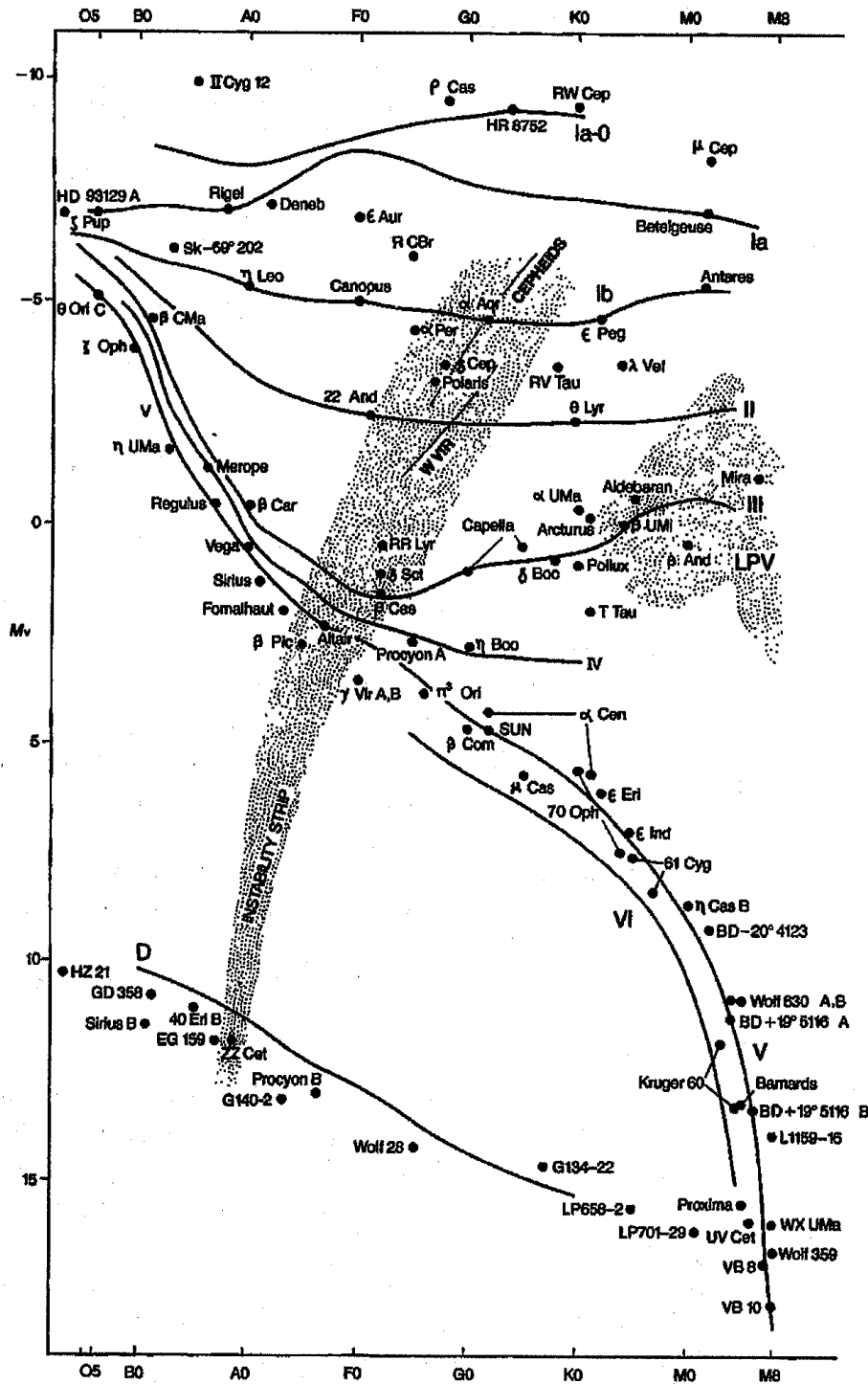
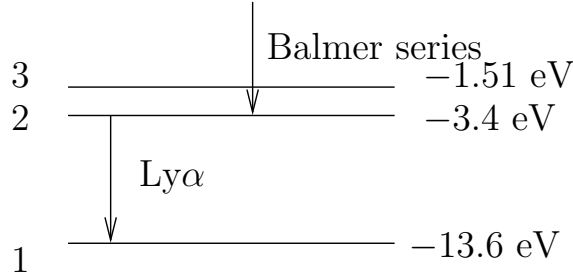


FIGURE 8.16 Luminosity classes on the H-R diagram. (Figure from Kaler, *Stars and Stellar Spectra*, © Cambridge University Press 1989. Reprinted with the permission of Cambridge University Press.)

23.6 Line series and edges

See spectra for an O and an A star above. Note "edge" feature in A star.

Reminder of the Balmer series:



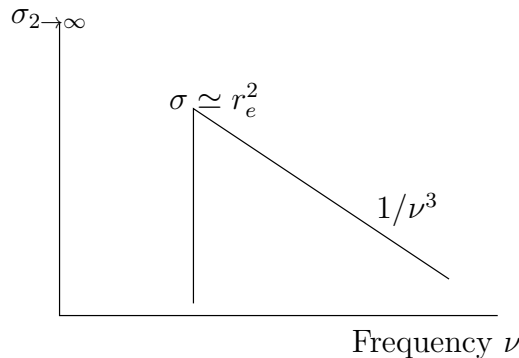
n	Lyman (to 1)	Balmer (to 2)
2	1215 (Ly α)	
3	1025 (Ly β)	6562 (3-2)
4		4861 (4-2)
5		4340 (5-2)
∞	911Å	3646

Lyman not seen much as it is absorbed by the ISM, the balmer edge is sharp if there is a lot of hydrogen in the first ionized state around.

So to see Balmer lines, we must have an appreciable number of H in the $n = 2$ state.

$$\frac{n_{n=2}}{n_{n=1}} = \exp\left(-\frac{10.2eV}{kT}\right) = 10^{-5} \text{ at } T = 10^4$$

"edge" from cross section:



at the transition $\sigma \simeq 10^{-16} \text{ cm}^2$, compared to $\sigma_{Thompson} \sim 10^{-24} \text{ cm}^2$. lots of optical depth.

So as long as

$$\exp\left(\frac{-10.2eV}{kT}\right) \frac{\sigma_\gamma}{\sigma_{Th}} \frac{n_H}{n_p} > 1$$

Balmer lines will be possible because the optical depth for photons capable of making either photo-ionization or transition have a large cross-section.

23.7 Opacity from H⁻ for cool stars

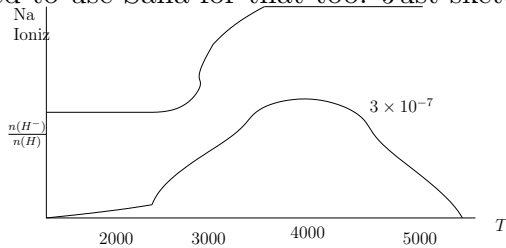
Below about 7,000-10,000 K, all hydrogen is neutral, most Alkali elements are singly ionized. This actually was a problem in understanding things for a while. H⁻ is a bound state of p+2e⁻. The second electron has binding 0.75 eV. This electron has a large orbital radius, so the cross section can be quite large even with low abundance. The free electrons needed to form H⁻ come from the alkali metals (Na,...) so we have e⁻ + H ↔ H⁻ + γ or μ_e + μ_H = μ_{H⁻} and so

$$\frac{n(H)}{n(H^-)} = \frac{n_{Q,e}}{n_e} \exp\left(-\frac{0.75\text{eV}}{kT}\right)$$

If all Alkali's are singly ionized n_e = 10¹³ cm⁻³ then

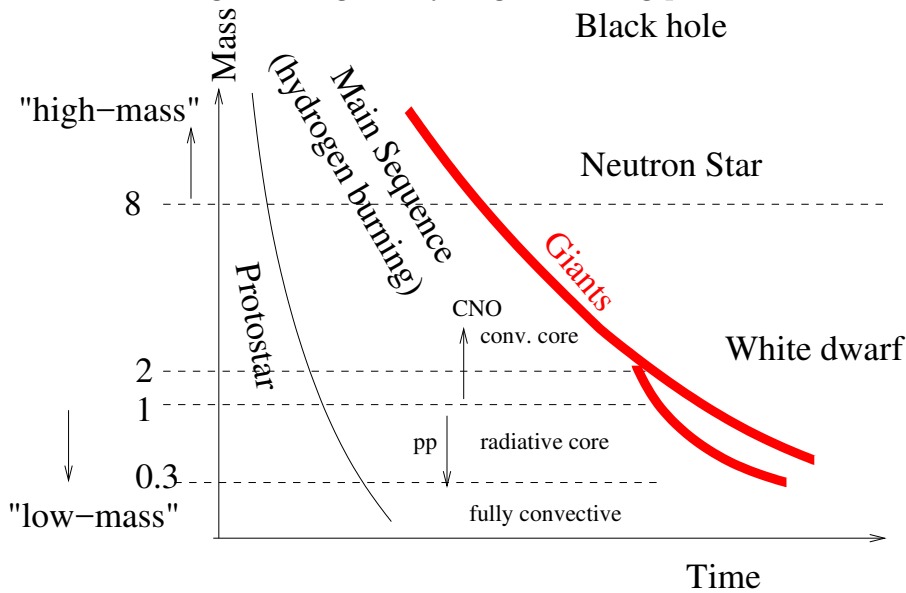
$$\frac{n(H)}{n(H^-)} = 10^{-8} \exp(8700/T)$$

note we'll run into trouble below 3000 since the alkali's won't be ionized. Would really need to use Saha for that too. Just sketch instead.



23.8 Evolution on the Main Sequence

How the star changes during the hydrogen burning phase.



Want to understand how the star changes its structure while still burning hydrogen. The main reason that this can be done is that there is a hierarchy of timescales. The time on the main sequence is

$$t_{MS} = \frac{E_{nuc}}{L} = \frac{E_{nuc}/m_p}{E_{th}/m_p} t_{KH}$$

since the evolution time on the main sequence is much longer than the Kelvin-Helmholtz time, the star evolves from one solution to another where each solution is in balance